Electronic Supplementary Information (ESI) for:

Plug-and-play assembly of paper-based colorimetric and electrochemical devices for multiplexed detection of metals

*Habdias A. Silva-Neto[a], Thiago M. G. Cardoso[a], Catherine J. McMahon[b], Lívia F. Sgobbi[a], Charles S. Henry[b] and Wendell K. T. Coltro[a,c,]**

[a] Instituto de Química, Universidade Federal de Goiás, 74690-900, Goiânia, GO, Brazil.

[b] Department of Chemistry, Colorado State University, 80523, Fort Collins, CO, USA.

[c] Instituto Nacional de Ciência e Tecnologia de Bioanalítica, 13083-861, Campinas, SP, Brazil

*Corresponding Author:

Professor Wendell K. T. Coltro

Instituto de Química, Universidade Federal de Goiás

Campus Samambaia, 74690-900

Goiânia, GO, Brazil

Fax: +55 62 3521 1127

E-mail: wendell@ufg.br

ORCID: http://orcid.org/0000-0002-4009-2291

Fabrication of microfluidic paper-based analytical devices (µPADs)

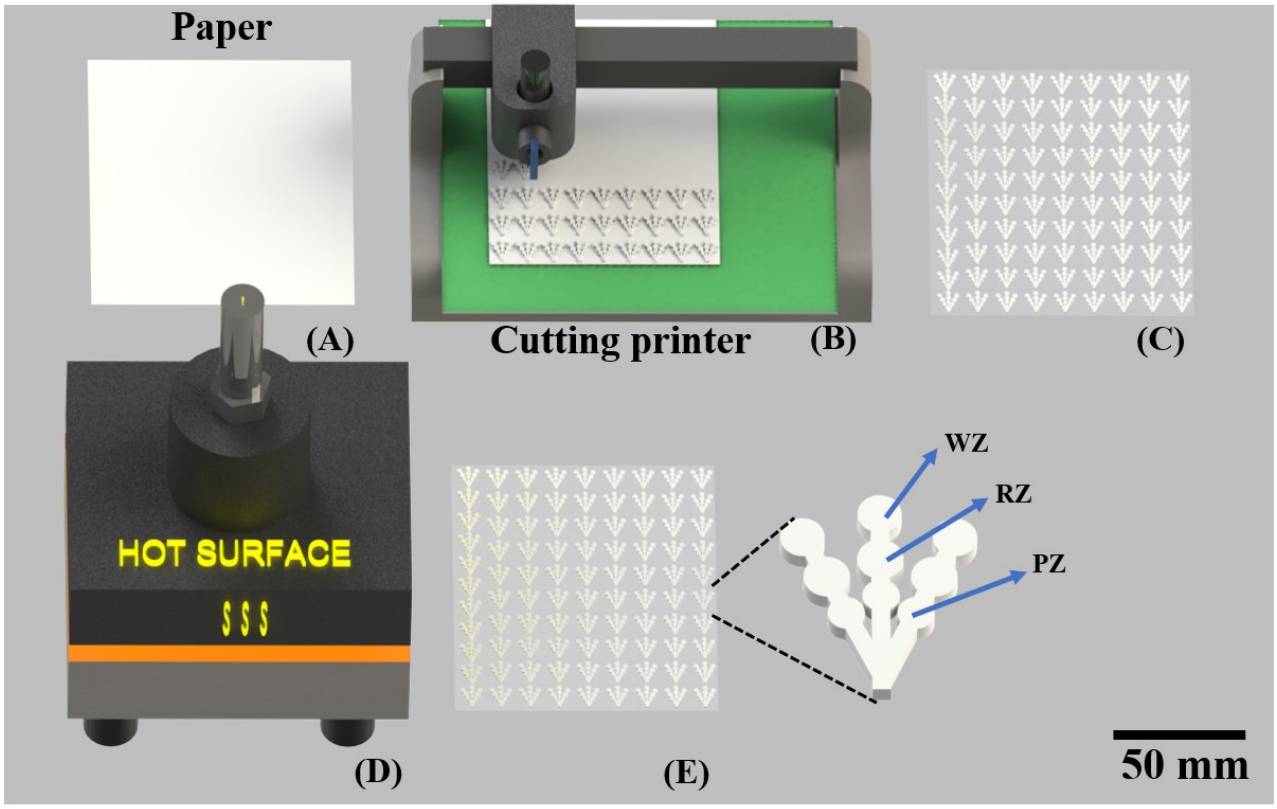

Fig. S1. Scheme of µPADs manufacturing using the cutting technique. Chromatographic paper (A); cutting process printer (B); devices cut out of thermal laminating sheet (C); thermal pressing for sealing devices (D); laminated µPAD ready for coupling to electrochemical device (E). In (E) the labels WZ, RZ and PZ indicate the waste, reaction and pre-treatment zones, respectively.

Fabrication of electrochemical paper-based analytical devices (ePADs)

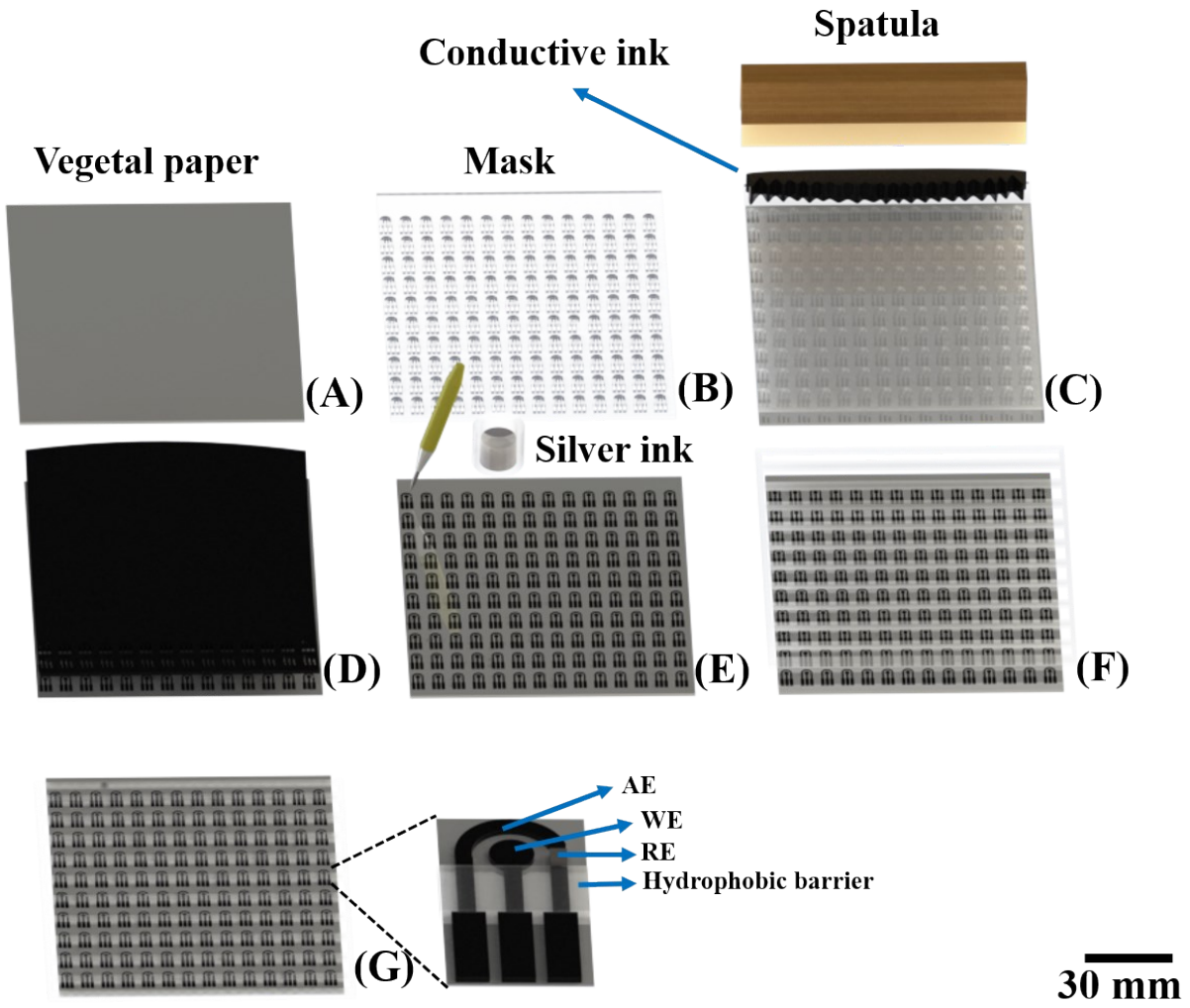

Fig. S2. Scheme of ePAD manufacturing using the screen-printing technique. Vegetal paper (A); plastic film containing electrode layout (B); laminated thermal laminating sheet mask on paper and addition of conductive carbon ink (C); filling the mask with conductive paint, curing for 30 s and removal of the plastic mold (D); pseudo reference electrode painted with silver ink (E); delimitation of the electroactive area of the electrode using hydrophobic barrier (F); laminated electrode ready for coupling to colorimetric device (G). The labels AE, WE and RE mean auxiliary, working and reference electrodes, respectively.

Identification of the sites for water sampling

Table S1. Identification and location of sampling along the Meia Ponte river course.

Site	Location
1	16º36'36.1"S; 49º16'59.1"W
2	16º37'41.1"S; 49º16'13.1"W
3	16º38'31.6"S; 49º15'24.1"W
4	16º39'11.3"S; 49º13'00.1"W

Optimization of the paper-based device fabrication

ePADs

As described in the main text, ePADs were fabricated by mixing different proportions of graphite, binder and MWCNT. Additionally, the best paper platform to support the fabrication of ePADs was also investigated. The criteria used to determine the best paper platform were the lowest charge transfer resistance in the electrochemical impedance spectroscopy (EIS), the peak current signal, and the oxidation/reduction ratio for the redox probe $[Fe(CN)_6]^{4-/3-}$ during cyclic voltammetry (CV). The performance of the simultaneous detection of Zn, Cd and Pb was also compared. According to the data presented in Fig. S3 and Table S2, the best electrochemical response was achieved using vegetal paper and the mixture of graphite, binder and MWCNT at ratio of 150:150:12 (in mass).

The CV and EIS measurements were carried out in 5 mmol L^{-1} $[Fe(CN)6]^{4-/3-}$ containing 0.1 mol L^{-1} KCl solution using a bipotentiostat/galvanostat model μStat 400 equipped with the DropView® software from DropSens S.L. (Oviedo, Spain) and a PGSTAT-100 potentiostat (Metrohm-Autolab, Netherlands) equipped with NOVA 2.1 software, respectively. For the EIS study, a sinusoidal signal at frequencies between 10^5 to 10^{-1} Hz and an amplitude potential of 20 mV was applied at 0.12 V (open-circuit potential).

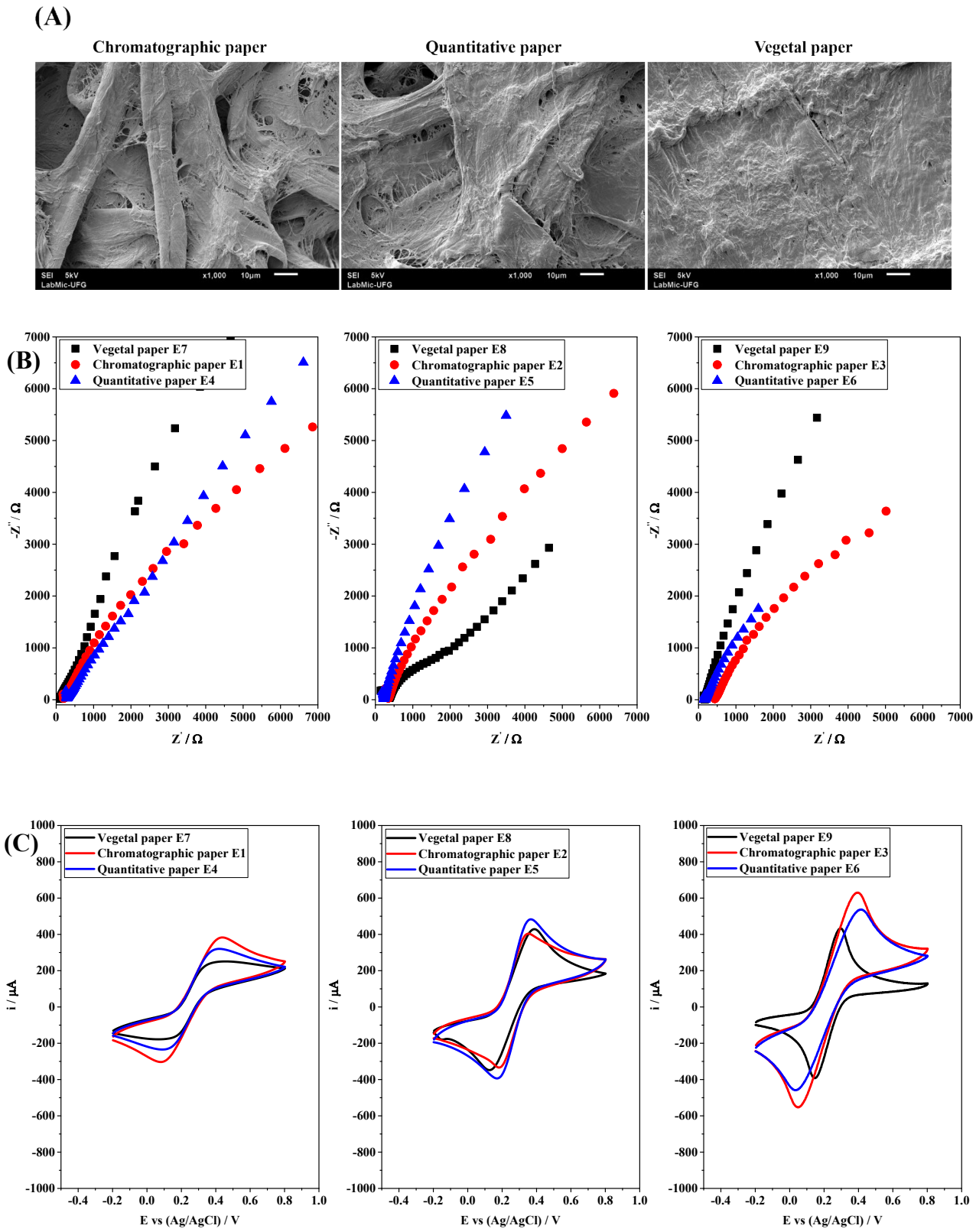
(A)
Chromatographic paper
Quantitative paper
Vegetal paper
SEI 5kV x1,000 10µm LabMic-UFG
(B)
Vegetal paper E7
Chromatographic paper E1
Quantitative paper E4
Vegetal paper E8
Chromatographic paper E2
Quantitative paper E5
Vegetal paper E9
Chromatographic paper E3
Quantitative paper E6
-Z'' / Ω
Z' / Ω
(C)
i / µA
E vs (Ag/AgCl) / V

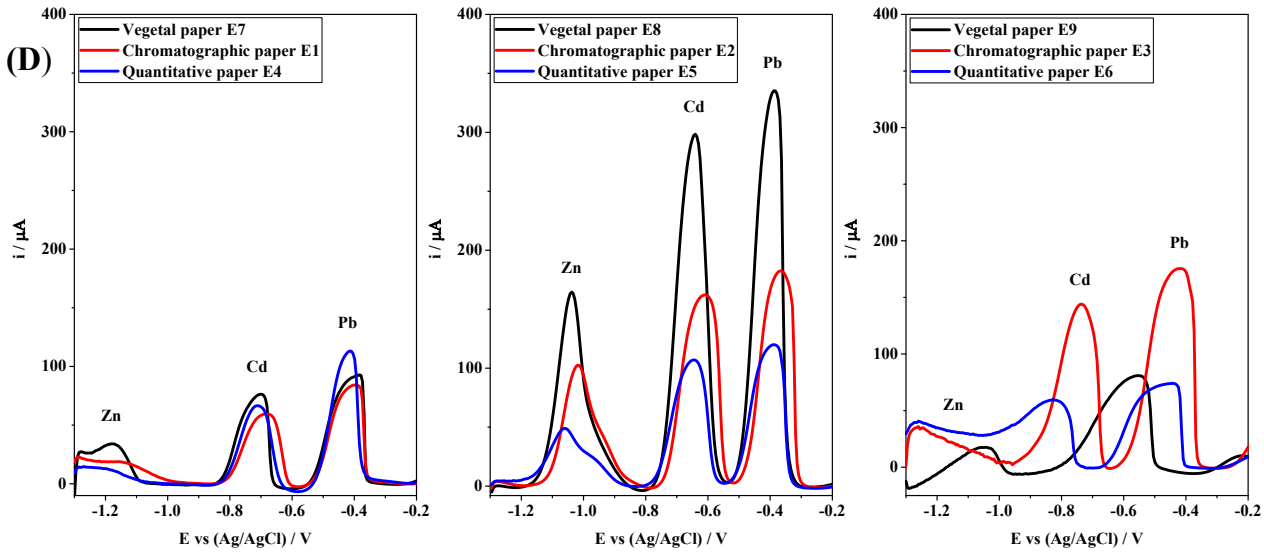

Fig. S3. SEM image of the different cellulose-based materials (A), electrochemical responses of the Nyquist plot in the EIS (B), CV (C) and SWASV (D) to ePAD using three graphite and binder proportions in different paper substrates.

Table S2. Optimization of ePAD fabrication, containing paper substrate, graphite to binder ratio and responses signals in CV, Nyquist plot in EIS and SWASV techniques using redox probe and a mixture of Zn(II), Cd(II), Pb(II) at 25 mg L^{-1}.

Parameters	**Paper Substrates**								
	Chromatographic			**Quantitative**			**Vegetal**		
ePAD	E1	E2	E3	E4	E5	E6	E7	E8	E9
Proportion[a]	50:250	150:150	250:50	50:250	150:150	250:50	50:250	150:150	250:50
i_{ap}/i_{cp}	1.06	0.87	1.05	1.13	1.10	1.04	1.12	1.06	1.14
ΔE_p (V)	0.34	0.16	0.34	0.3	0.19	0.38	0.25	0.24	0.14
R_{ct} (kΩ)	14.5	29.9	13.1	14.0	42.7	15.4	34.3	2.6	1.4
R_s (kΩ)	0.33	0.22	0.44	0.30	0.18	0.17	0.34	0.36	0.15
i_{Zn} (μA)	1	101	*	1	49	*	15	164	18
i_{Cd} (μA)	59	161	143	66	107	59	75	300	81
i_{Pb} (μA)	84	181	176	112	120	73	93	337	11

[a]Graphite to binder ratio; E= electrochemical sensor; * No signal

Table S3

Parameters optimized for electrochemical detection.

Parameter	Bismuth film		SWASV	
	Range	Optimized	Range	Optimized
Deposition potential (V)	-0.6 to -1.1	-0.9	-1.3 to -1.6	-1.4
Time potential (s)	50 to 200	150	125 to 200	150
Frequency (Hz)	-	-	1 to 25	15

In addition, the bismuth film (*ex-situ*) and square wave anodic stripping voltammetry (SWASV) conditions for Zn, Cd and Pb detection were also evaluated (Table S3). The characterization of the ePADs fabricated under the optimized conditions was performed through CV and field-emission gun scanning electron microscopy (FEG-SEM), the results are displayed in Figs. S4 and S5.

The FEG-SEM was performed with a JEOL microscope (model JSM-7100F, Waltham, MA, USA) with resolution 1.2 to 2.0 nm and power 1.0 to 30 kV, used to characterize the electrode surface modified with bismuth and MWCNTs.

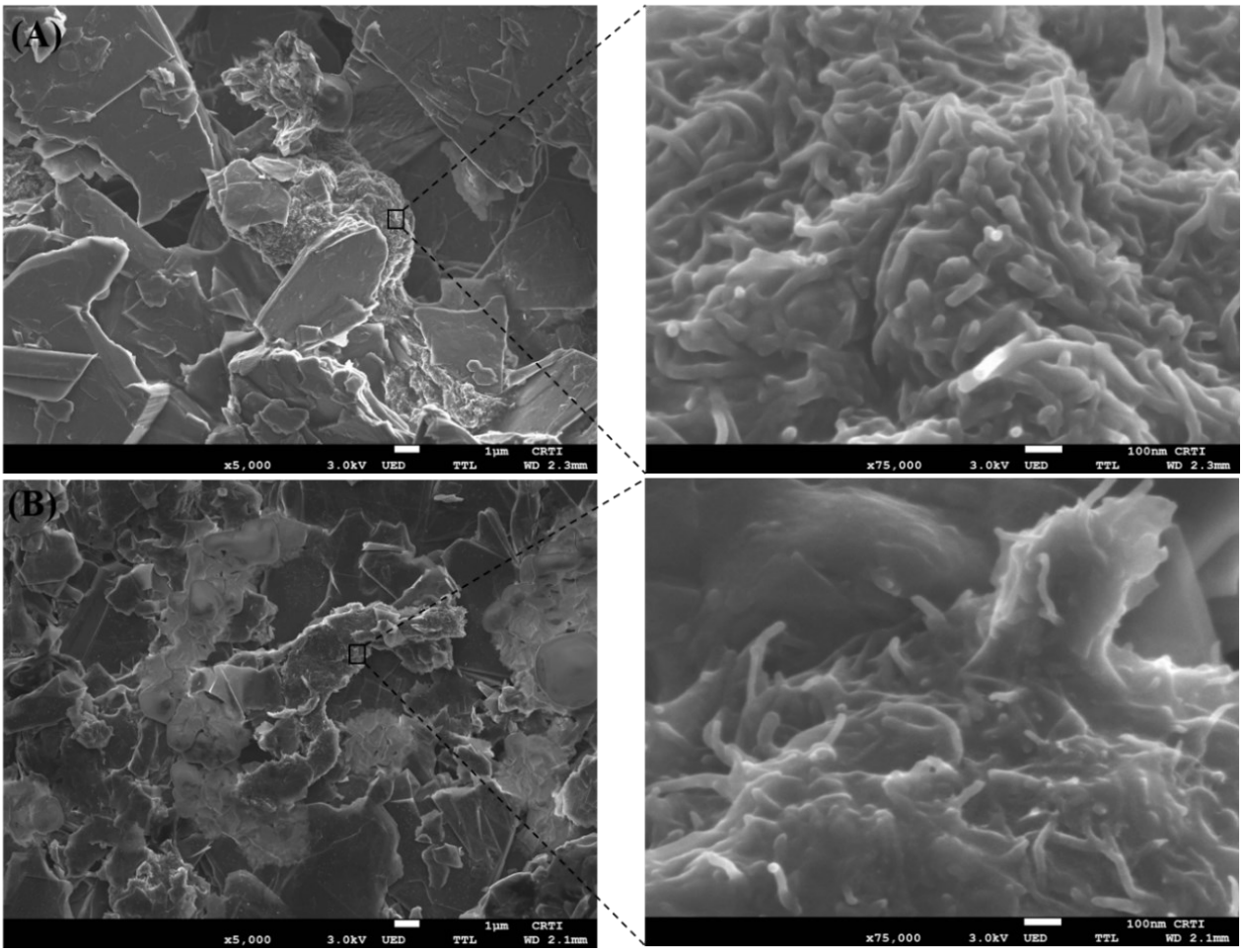

Fig. S4. FEG-SEM showing the working electrode surface (A) before and (B) after modification with bismuth. Images were recorded at magnitudes of 1000x (left) and 75000x (right).

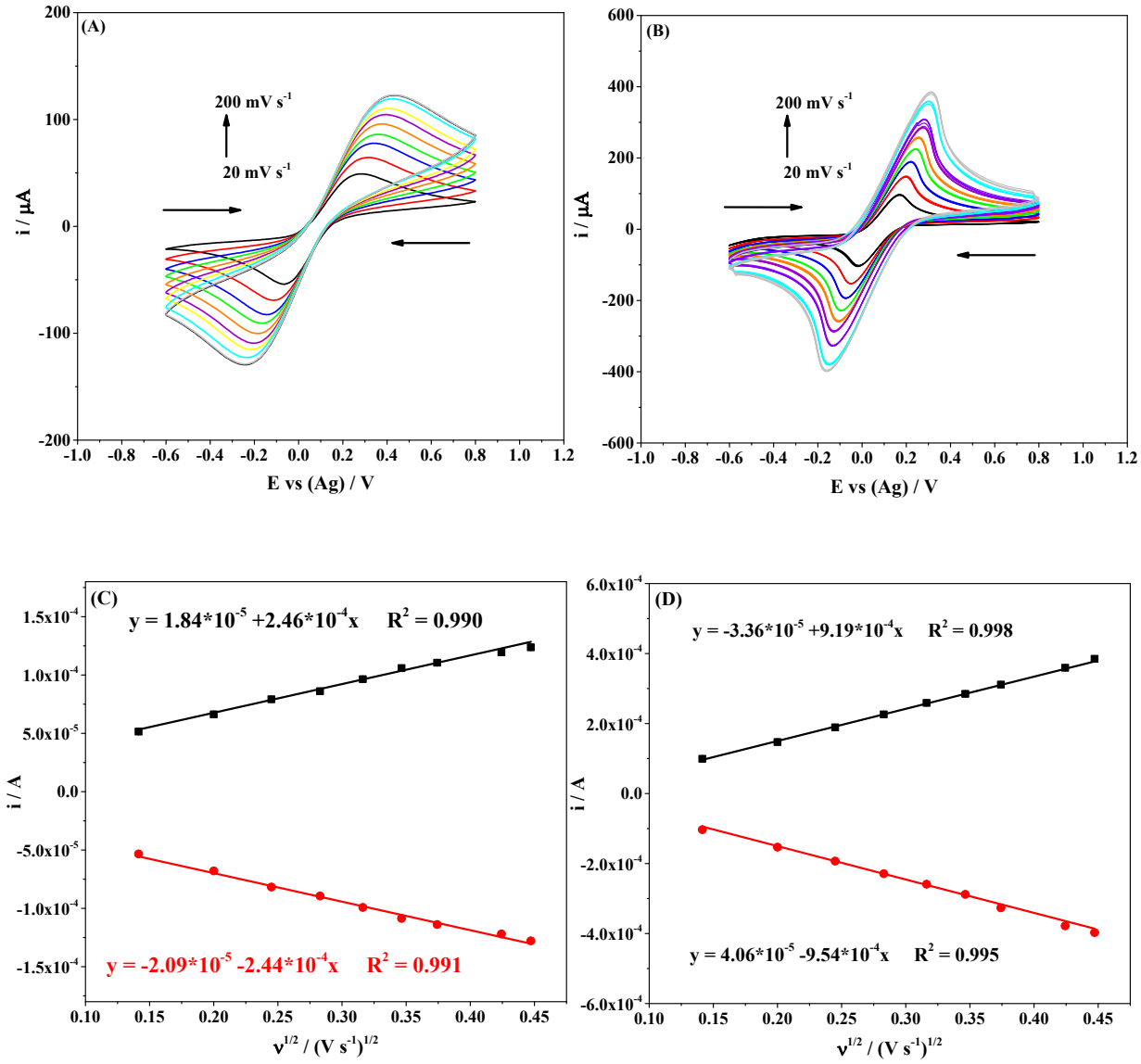

Fig. S5. (A, B) Cyclic voltamograms recorded at scan rates from 20 to 200 mV s^{-1} for a redox probe composed of 5.0 mmol L^{-1} $[Fe(CN)_6]^{4-/3-}$, prepared in 0.1 mol L^{-1} KCl, and (C, D) the respective plots showing the peak current against square root of scan rate. The data were recorded using (A, C) unmodified electrodes and (B, D) bismuth-modified electrodes. The electroactive areas for umodified and modified electrodes were 0.069 and 0.272 cm^2, respectively (n = 3).

µPAD

For the fabrication of µPADs, the design, type of paper substrate, zone diameter size, size of the microfluidic channel, and color channel were evaluated. Three paper types (chromatographic grade 1, quantitative grade 40 (porous size 25 µm) and quantitative grade 42 (porous size 2.5 µm)) were evaluated for fabricating the µPADs due to their different specifications including porous size,

thickness, particle retention, filtration and wicking speed.[1] For this investigation, the signal-to-noise ratio and the color uniformity of the pixel intensity were thoroughly evaluated. Considering the data presented in Figs. S6-S10, the best analytical responses were achieved when using a tree-shape channel design printed on chromatography paper, 3 mm of diameter zone, 12 mm of microfluidic channel, and color channel yellow for Cu and magenta (Fe and Ni). The optimized experimental results are summarized in Tables S4 and S5.

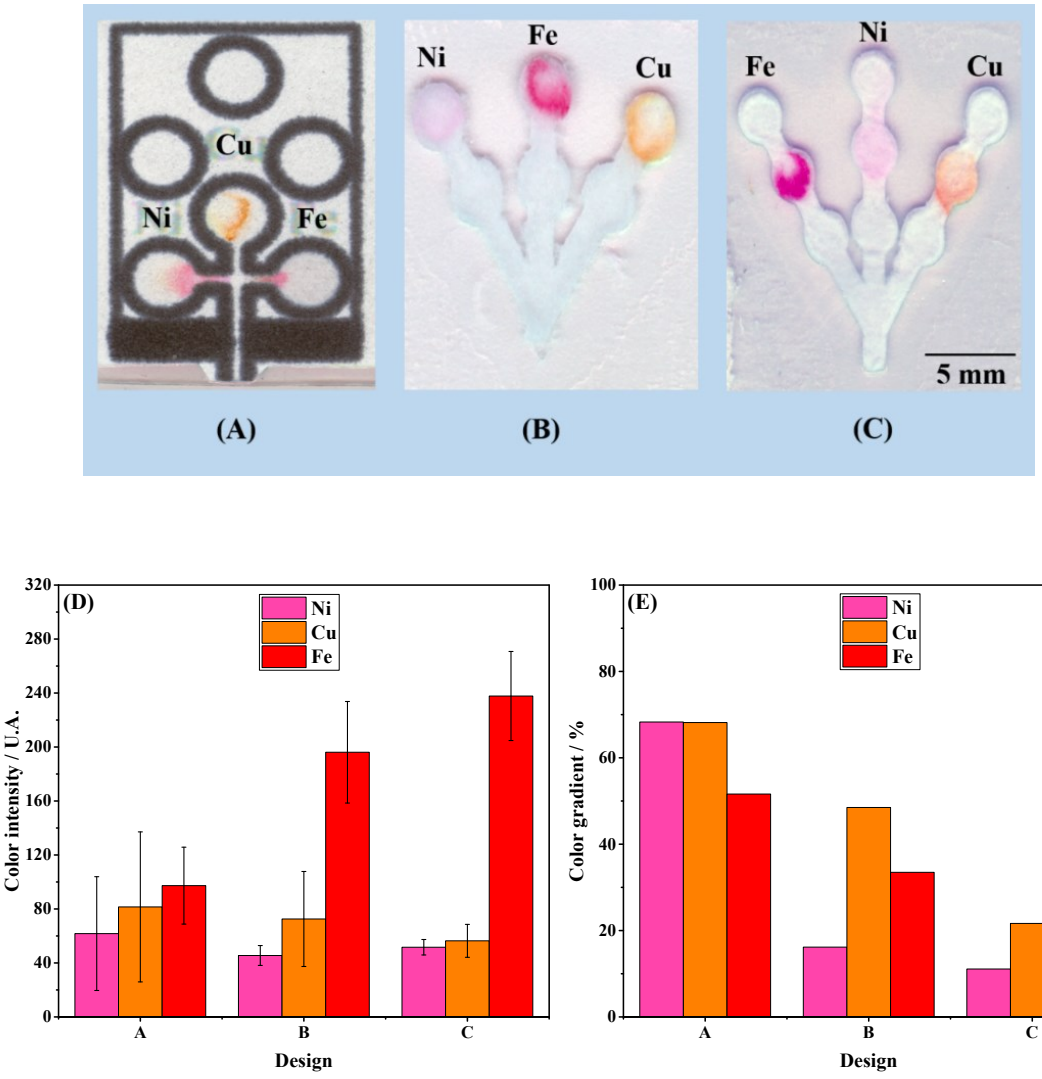

Fig. S6. Optimization of the device design, using wax barriers (A); barrier-free and pretreatment zones (B); barrier-free, pretreatment and disposal zones (C); the color intensity (D) and RSD of color gradient (E). Using assay with Fe(II), Ni(II) and Cu(II) at 25 mg L^{-1} (n=3).

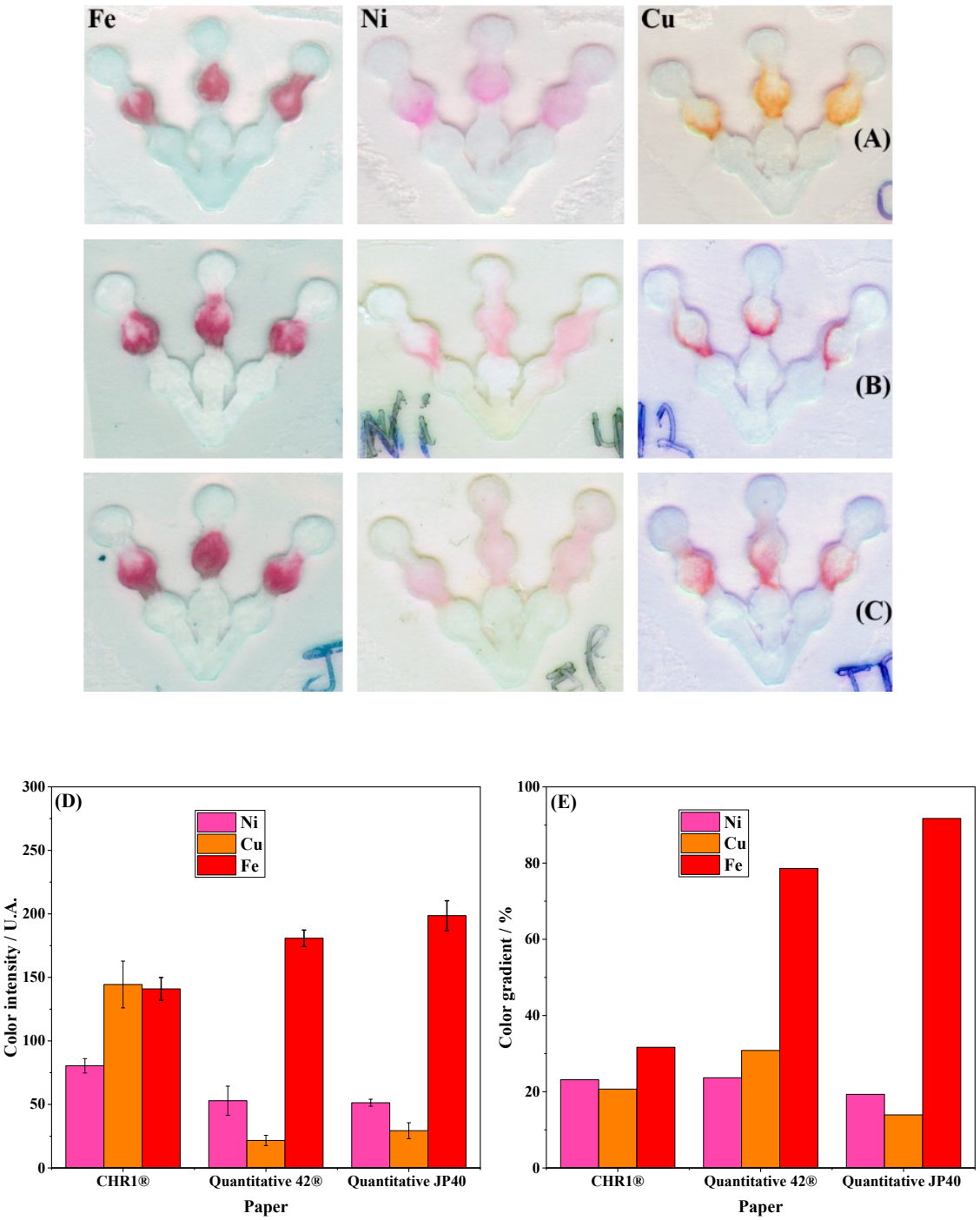

Fig. S7. Optimization of paper substrate, chromatography paper (A); Quantitative paper (B); JP42 quantitative paper (C); the color intensity (D) and RSD of color gradient (E) based on the assay with Fe(II), Ni(II) and Cu(II) at 25 mg L^{-1} (n=3).

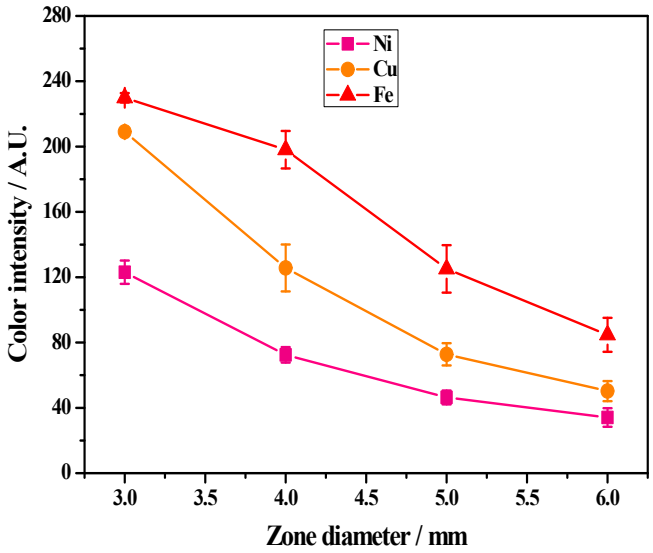

Fig. S8. Behavior of the color intensity of Ni, Cu and Fe assays varying the zone diameter from 3 to 6 mm based on the assay with Fe(II), Ni(II) and Cu(II) at 15 mg L^{-1} (n=6).

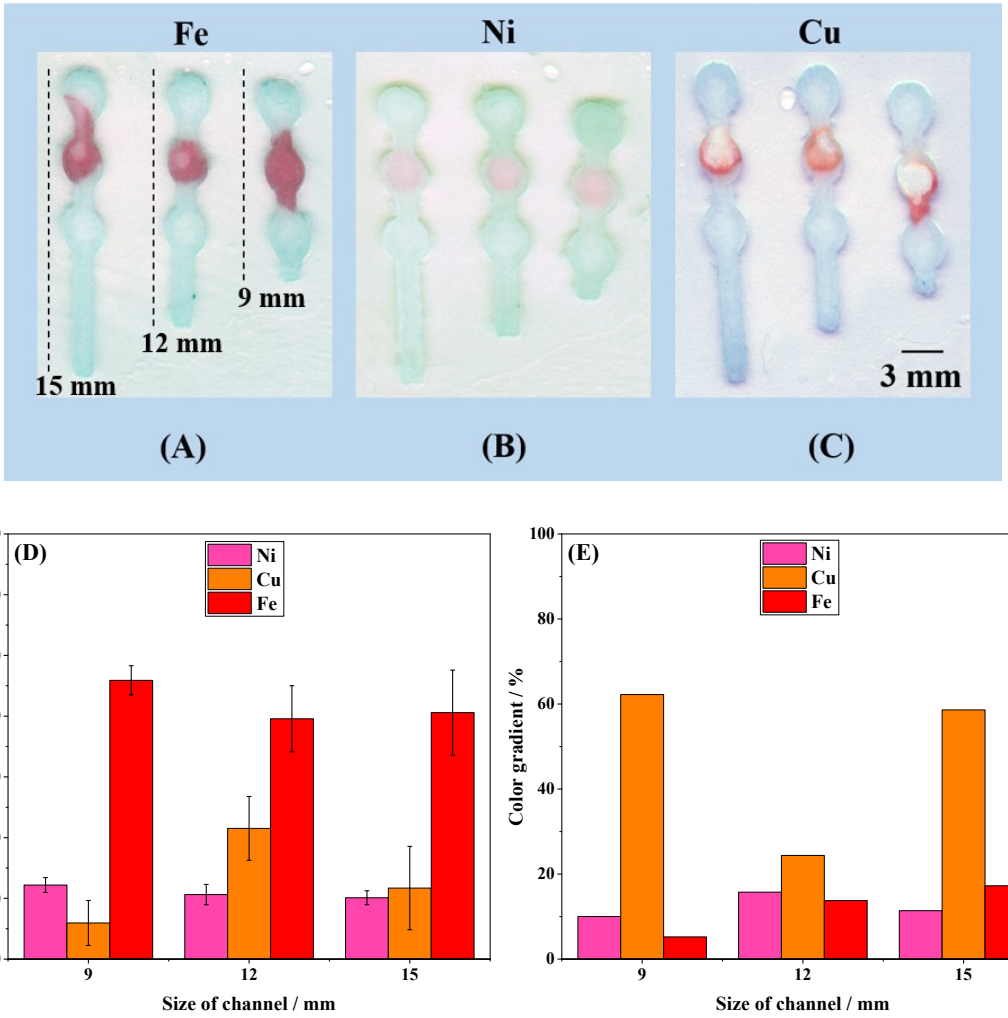

Fig. S9. Optimization of channel size using 9.0 to 15.0 mm range . Fe assay (A); Ni assay (B); Cu assay (C); the color intensity (D) and RSD of color gradient (E). The assay was optimization using Fe(II), Ni(II) and Cu(II) at 25 mg L^{-1} (n=3).

Table S4. Parameters optimized for colorimetric detection.

Parameter	Range	Optimized
Color channel (color intensity)	CMYK to RGB	Yellow for Cu, magenta (Fe and Ni)
Zone diameter (mm)	3.0 to 6.0	3.0
Channel length (mm)	9.0 to 15	12

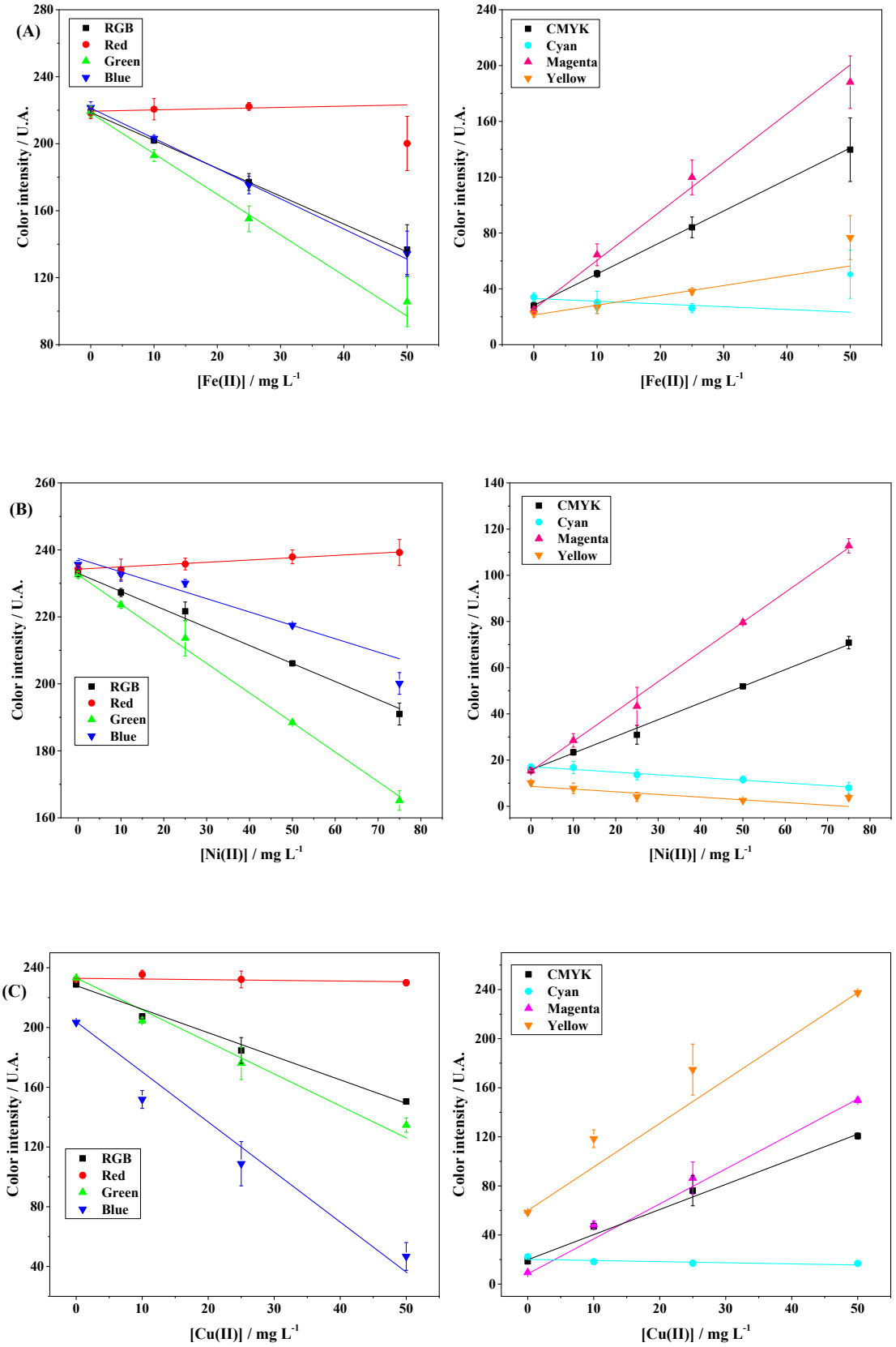

Fig. S10. The calibration curves at 5 to 75 mg L^{-1} range for RGB and CMYK systems to optimize the color channel in the colorimetric assays of Fe (A), Ni (B) and Cu (C) (n=3).

Table S5. The parameters to optimize the color channel for the colorimetric assays of Fe, Ni and Cu using Fig. S8. For the analytical curve at 5 to 75 mg L^{-1} range using RGB and CMYK color systems.

Assay	Parameter	Color channel							
		RGB	Red	Green	Blue	CMYK	Ciano	Magenta	Yellow
Fe	b	-1.66	0.08	-2.42	-1.81	2.25	-0.19	3.51	0.71
	R^2	0.99	0.36	0.99	0.99	0.99	0.03	0.99	0.89
Ni	b	-0.54	0.07	-0.88	-0.39	0.72	-0.12	1.29	-0.12
	R^2	0.99	0.96	0.99	0.94	0.99	0.98	0.99	0.66
Cu	b	-1.57	-0.04	-2.13	-3.34	2.07	-0.09	2.81	3.58
	R^2	0.99	0.02	0.96	0.95	0.99	0.37	0.99	0.99

b= slope

Estimative of the cost to the integrated paper-based device

The cost of the integrated device was estimated using the different paper types and the amount of material required to prepare the electrodes and the polymeric film. Table S6 summarizes the cost of all required consumables.

Material	Amount	Cost per sheet paper *ca*. (US$)	Cost per device *ca.* (US$)
Vegetal paper (A4)	1	0.40	0.007
Graphite Powder (g)	3.0	0.14	0.001
Carbon nanotube (g)	0.02	0.80	0.010
Binder (g)	3.0	0.18	0.001
Thermosensitive polyester film (A4 size)	2	0.80	0.005
Silver paint (g)	0.02	0.20	0.001
CHR1® paper (200x200) mm	1	0.60	0.007

Table S6. Cost in dollars per manufacturing the multiplex analytical device.

* cost per ePAD *ca*. (US$) = 0.007 + 0.001 + 0.01 + 0.001 + 0.005 + 0.001 = 0.02

* cost per µPAD *ca*. (US$) = 0.007

* cost per multiplex device *ca*. (US$): 0.03

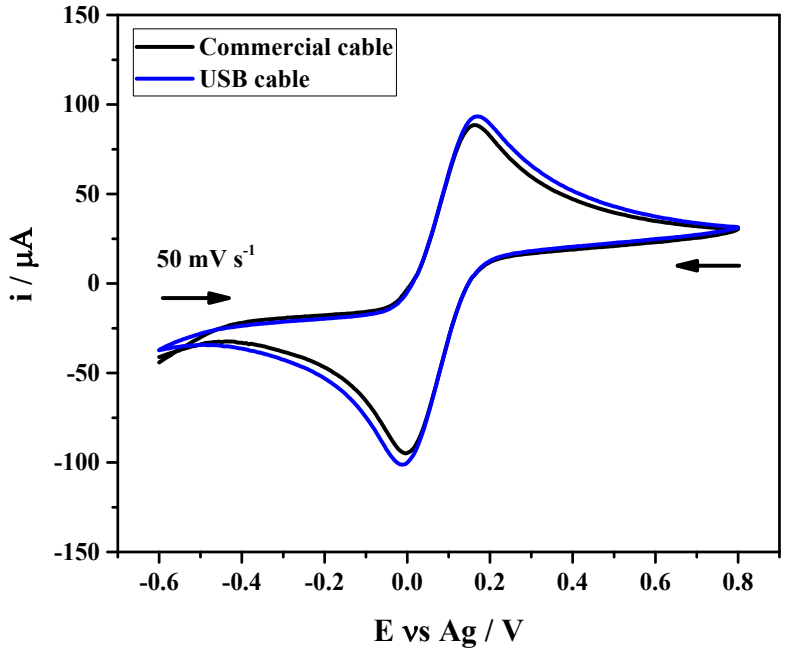

Fig. S11. Comparison of voltammetric behavior performed with ePAD connected through alternative and commercial cables using 5.0 mmol L^{-1} redox probe $[Fe(CN)_6]^{4-/3-}$ in 0.1 mol L^{-1} KCl at 50 mV s^{-1}.

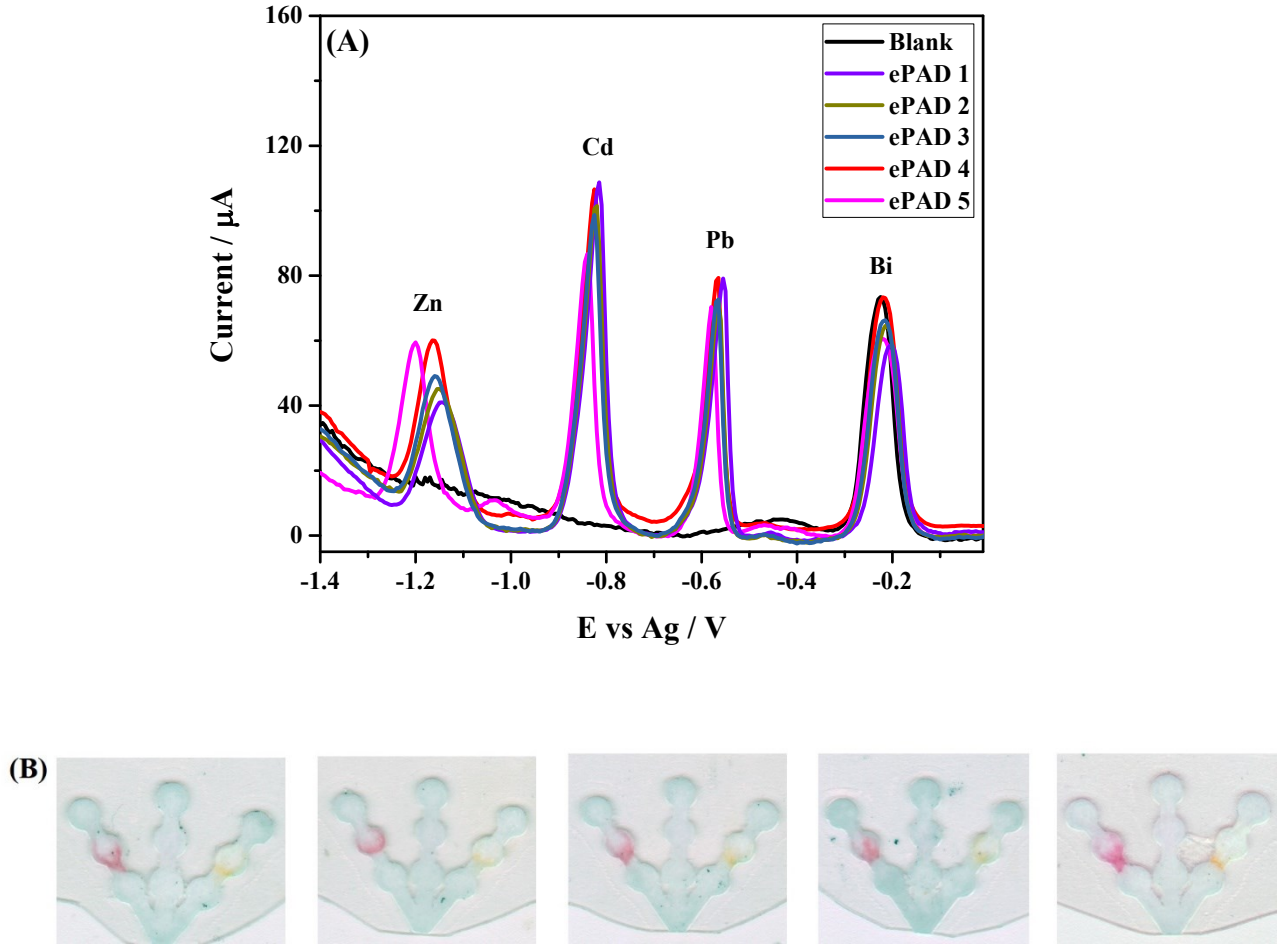

Fig. S12. (A) Voltammograms recorded for the reprodutibility study of Bi/ePADs using a mixture of Zn(II), Cd(II) and Pb(II) (n=5); (B) optical images showing the reproducibility for colorimetric assay using a mixture of Fe(II), Ni(II) and Cu(II) (4 mg L^{-1} each) (n = 5).

Table S7. Metals concentrations in a water sample river (2nd location) and the recovery study, after the standard addition method.

Metal	Found (μg L^{-1})	Added (μg L^{-1})	Found (μg L^{-1})	Recovery (%)
Zn	<LOD	200	182 ± 10	91.2
Cd	16.1 ± 0.6	200	221 ±13	110.3
Pb	102 ± 9	200	297 ±15	98.5
Fe	166 ± 11	2000	1683 ± 95	76.5
Ni	<LOD	2000	2421 ± 140	121.1
Cu	<LOD	2000	1937 ± 120	102.8

Notes and references

1 E. Evans, E. F. Moreira Gabriel, W. K. Tomazelli Coltro and C. D. Garcia, *Analyst*, 2014, **139**, 2127–2132.